Chapter 10
Modal Testing of James Webb Space Telescope (JWST) Optical Telescope Element (OTE)

Douglas J. Osterholt, David Cloutier, Timothy Marinone, and Reem Hejal

Abstract A modal survey was conducted on the James Webb Space Telescope optical telescope element (OTE) to obtain dynamic characterization of the system to be used in finite element model validation and loads assessments. Modal testing was performed by ATA Engineering, Inc., (ATA) and Northrop Grumman Systems Corporation (NGSC) for two configurations (stowed and deployed), which are representative of the launch and on-orbit orientations, respectively. The modal test of the OTE is essential in order to correlate and update the finite element model (FEM) that will be used for predicting launch loads and on-orbit performance, including wave-front error and line-of-sight calculation for optimal performance. Fixed base testing was conducted for both configurations. Pretest analysis activities were performed by NGSC, and testing was performed by ATA. Unanticipated flexibility in the stowed configuration fixture necessitated additional testing and analysis to validate the model boundary condition. The deployed configuration testing was successfully performed with 188 modes extracted up to 100 Hz. This paper provides details on the overall test effort and insight into the performance of a modal test on complex spacecraft flight hardware with high modal density.

Keywords Modal survey • Mode enhancement • Fixed base • Spacecraft

Abbreviations

ATA	ATA Engineering, Inc.
CMIF	Complex mode-indicator function
DOF	Degree of freedom
FEM	Finite element model
FRF	Frequency response functions
Hz	Hertz
IMAT	Interface between MATLAB, analysis, and test
JWST	James Webb space telescope
MAC	Modal assurance criteria
MMIF	Multivariate mode-indicator function
NGSC	Northrop Grumman Systems Corporation
OSS	OTE support structure
OTE	Optical telescope element
PSMIF	Power spectrum mode-indicator function
RMS	Root mean square
TAM	Test analysis model
TDM	Test display model
TEDS	Transducer electronic data sheet

D.J. Osterholt (✉) • D. Cloutier • T. Marinone
ATA Engineering Inc., 13290 Evening Creek Drive South, Suite 250, San Diego, CA 92128, USA
e-mail: doug.osterholt@ata-e.com

R. Hejal
Northrop Grumman Systems Corporation, Aerospace Systems, One Space Park, Redondo Beach, CA 90278, USA

A. Brandt, R. Singhal (eds.), *Shock & Vibration, Aircraft/Aerospace, Energy Harvesting, Acoustics & Optics, Volume 9*,
Conference Proceedings of the Society for Experimental Mechanics Series, DOI 10.1007/978-3-319-30087-0_10

10.1 Introduction

Spacecraft models are becoming larger and more complex every year. Performing a modal test on the full assembly can be challenging and require significant resources. To reduce risk and cost, detailed modal tests of subassemblies are being performed to improve high-fidelity models that can be used with confidence in the final assembly. The challenge, in this case, was to accurately measure a modally dense structure up to higher frequencies than similar modal test programs in the past.

NASA is developing a next-generation space telescope, the James Webb Space Telescope (JWST), and Northrop Grumman Systems Corporation (NGSC) is building the optical telescoping element (OTE). As part of the development, a FEM was built for loads assessment and optical performance, or line of sight. A modal survey was performed to obtain the dynamic characteristics of the OTE and will be used to correlate and update the FEM. ATA Engineering (ATA) performed the modal survey of the JWST OTE in two fixed base configurations: stowed and deployed. These two configurations represent the launch and on-orbit orientations of the JWST. This structure has many modes in the frequency band of interest, which provides a unique challenge in test planning, performance, and data analysis.

The JWST OTE, shown in Fig. 10.1 in the stowed configuration and in Fig. 10.2 in the deployed configuration, has dimensions of 3 m × 4 m × 8 m when stowed and dimensions of 10 m × 6 m × 10 m when deployed. The deployed configuration was mounted to the OTE support structure (OSS), which consists of a large frame structure and the struts used to connect to the OTE. The deployed configuration also utilized tuned mass dampers (TMDs) mounted to the three main struts. These small TMDs were mounted to minimize the lateral motion of the struts in the 6 Hz frequency range; 9.5 Hz TMDs were also evaluated but are not discussed in this paper.

The objectives of the modal survey were to measure transfer functions up to 250 Hz and identify all primary structural modes below 50 Hz in the stowed configuration and significant modes below 100 Hz in the deployed configuration.

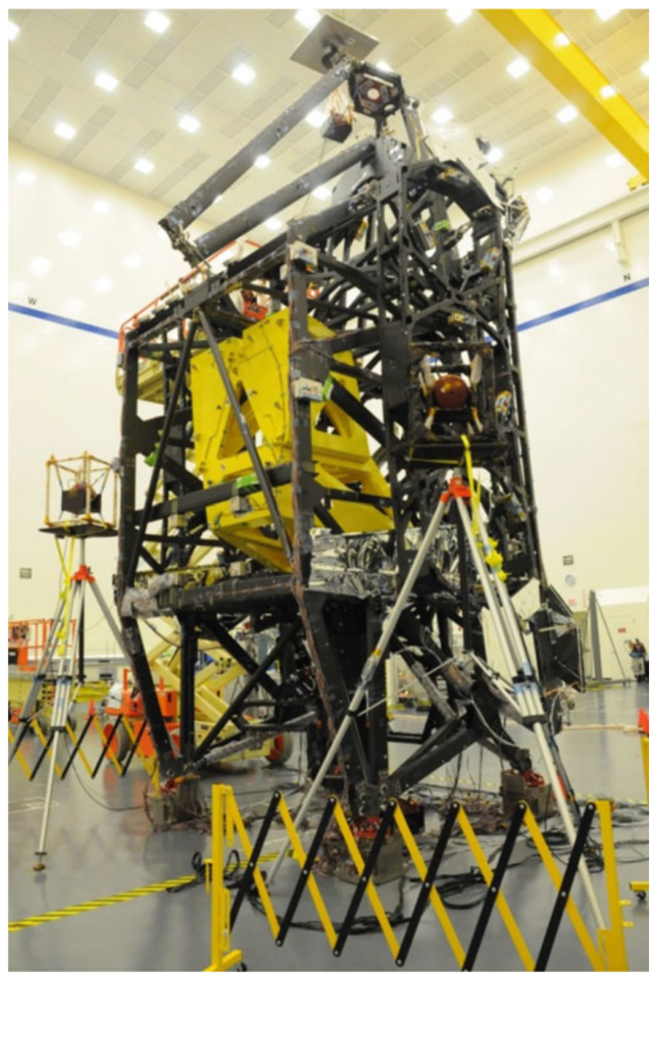

Fig. 10.1 JWST OTE stowed configuration

Fig. 10.2 JWST OTE deployed configuration

This majority of the modal analysis focused on the deployed configuration; however, both the deployed and stowed configurations are discussed in this paper. For the deployed configuration, the analysis predicted a total of 349 modes below 100 Hz. Many of these modes were local modes that are not of interest. The final test results were 188 structural modes below 100 Hz. The stowed configuration presented its own challenge in that the fixture did not provide an ideal boundary condition; one direction was less stiff than predicted, so static testing was performed to verify and update the model boundary condition.

10.2 Pretest Analysis

Northrop Grumman performed a pretest analysis to identify the required accelerometer locations and directions. The final set of measurement locations for the stowed configuration totaled 341 fixed degrees of freedom (DOF) at 145 node locations. The final set of measurement locations for the deployed configuration totaled 354 fixed DOF at 151 node locations. The test measurement DOF were used to make a test display model (TDM). This model, used for visualizing the mode shapes, consists of nodes and "dummy" elements. The TDM is shown for the stowed configuration in Fig. 10.3 and for the deployed configuration in Fig. 10.4, where each arrow represents a DOF or accelerometer. A large number of channels represent the primary mirror bays. These measurements are important for on-orbit performance evaluation of the telescope.

The pseudo-orthogonality for the deployed configuration showed that the test measurements do a good job of describing the mode shapes up to approximately 50 Hz. Above 50 Hz the modes were identified but with the limited number of accelerometers, unique mode shapes could not be described. Once the pretest analysis was finalized, the test analysis model (TAM) was computed using Guyan reduction. The TAM consists of the mass, stiffness, and constraint matrices. These were used to perform cross-orthogonality and back-expansion during the test. The back-expansion uses the TAM constraint matrix to interpolate missing DOF for purposes of visualization only.

10.3 Test Performance

The first challenge with setup of this test was cleaning all the equipment and cables to accommodate space flight hardware in a 10 k clean room. Every cable had to be scrubbed by hand. Installation required using superglue and two layers of Kapton tape for attachment of the accelerometers and blocks. Barcodes and TEDS technology were used to map the channels to the finite element model node numbers [1]; using the FEM nodes as the test measurement locations removes any steps to map from test to analysis to perform cross-orthogonality and cross-modal assurance criteria (cross-MAC) calculations. The accelerometer installation was performed by ATA personnel in parallel with NGSC personnel performing final hardware

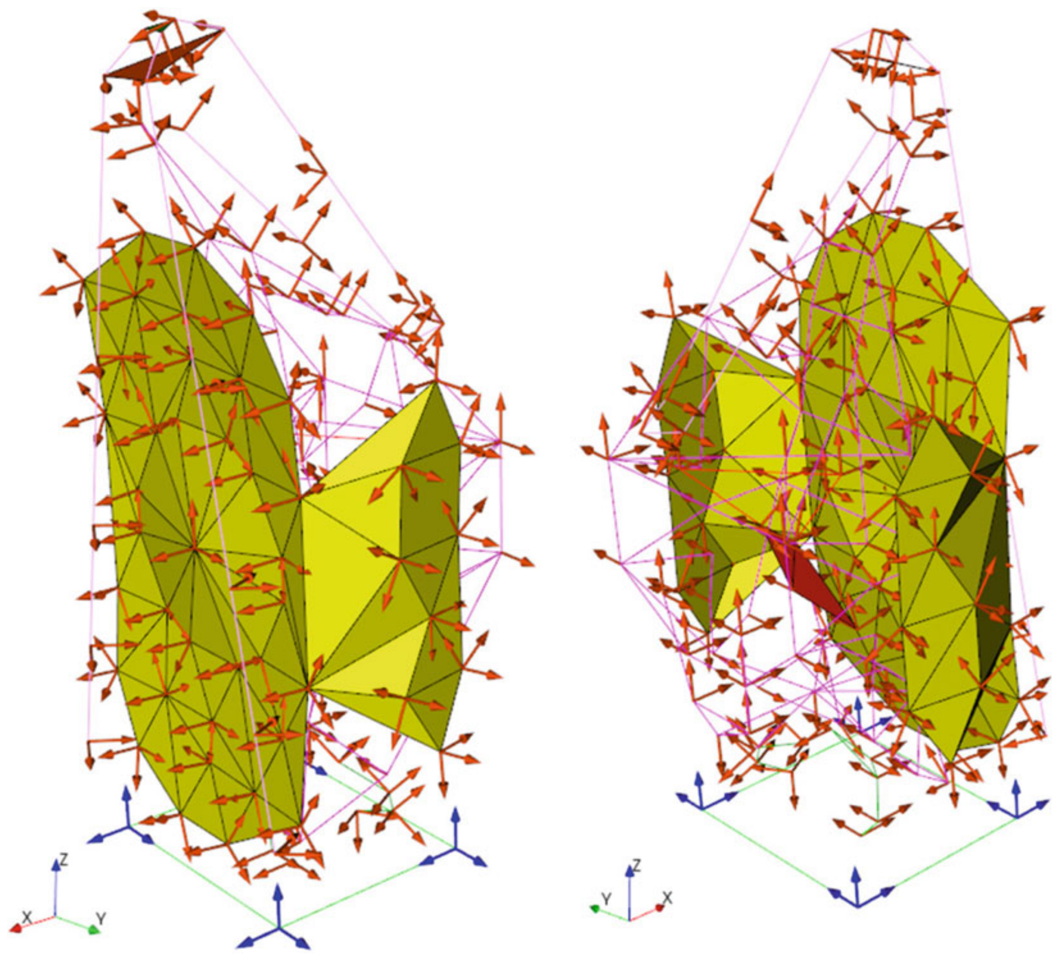

Fig. 10.3 JWST OTE TDM with measurement locations in the stowed configuration

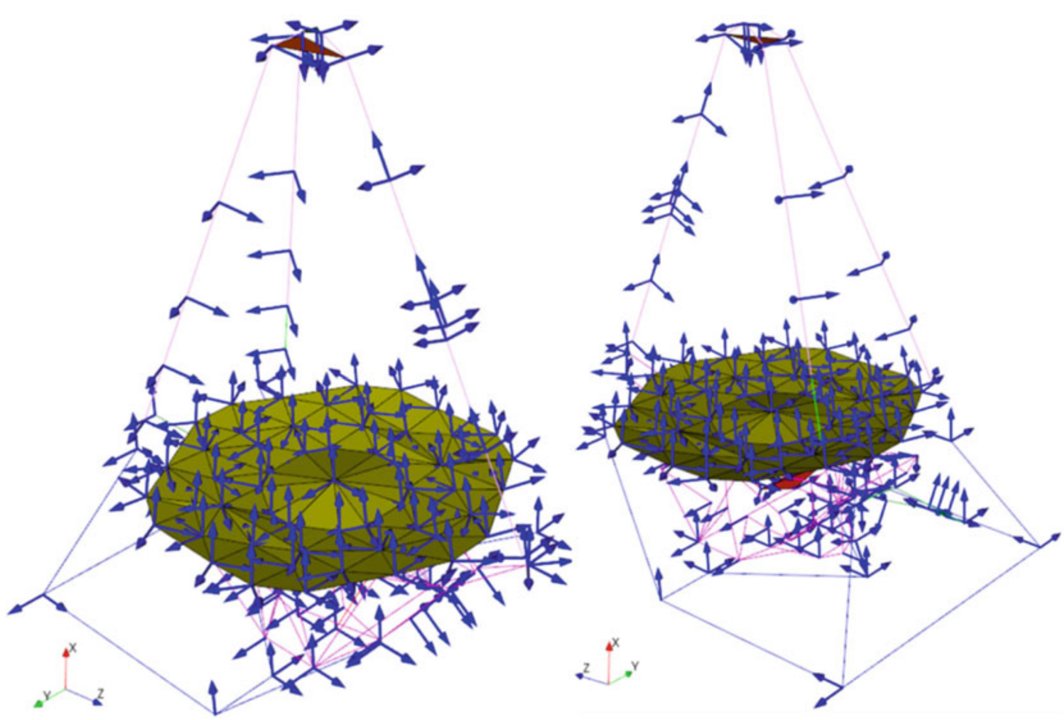

Fig. 10.4 JWST OTE TDM with measurement locations in the deployed configuration

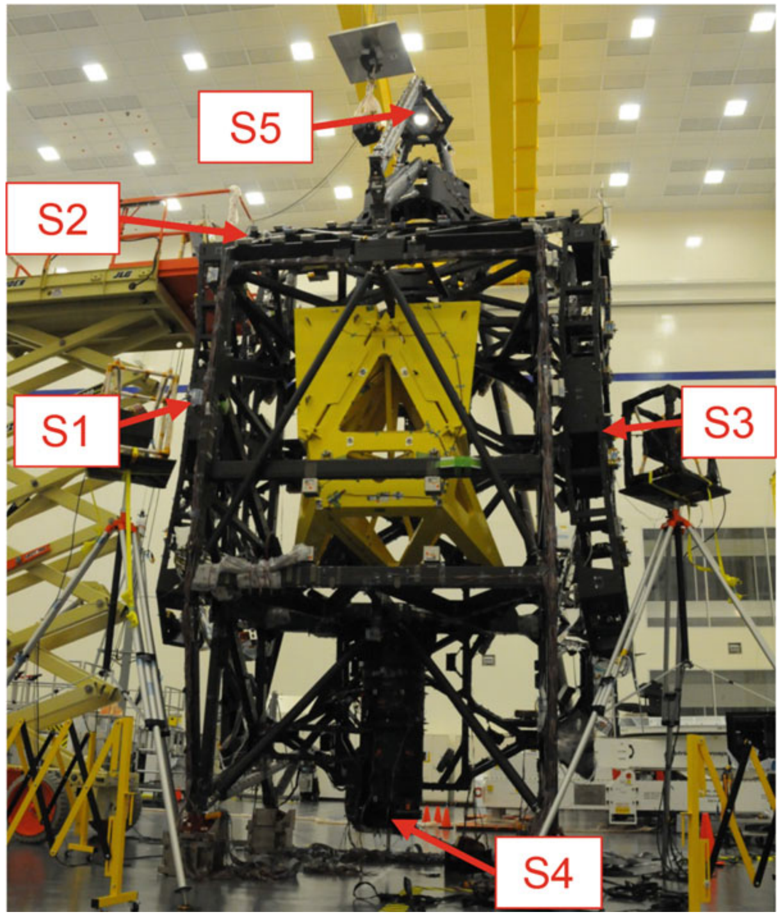

Fig. 10.5 Stowed configuration shaker locations

configuration. A majority of the accelerometers were installed in local coordinate systems to allow accurate orientation. The installation of accelerometers, cables, and shakers was done intermittently over a 6-day period.

Shakers were selected using the analysis predictions to excite all the modes in a single setup. The stowed configuration utilized five Modal-110 shakers and is shown in Fig. 10.5. The deployed configuration utilized seven Modal-110 shakers and is shown in Fig. 10.6, which provides a front and side view of the deployed configuration. The shakers were supported using suspension cages and a variety of support stands and one overhead crane. Since the test article boundary condition was fixed, the shakers were supported in a free-free boundary condition. Most of the stands used were provided by ATA and consist of modified tripods allowing easy adjustment and alignment.

Test performance started with ambient background noise checks and a linearity assessment at each shaker location. Linearity was assessed using multiple force levels. The "best" force level, based upon data quality, for each shaker was then used in a multi-reference burst-random run. For the stowed configuration, the best levels ranged from 1.5 to 7 lbs RMS. Some locations were lower because they were attached to flexible points while others were at hard points. The deployed configuration required lower force levels and ranged from 0.5 to 3 lbs RMS. All the data sets were recorded with a maximum frequency of 250 Hz (sample rate of 640 Hz) and processed with a delta F of 0.029 Hz to provide accurate resolution for observing modes throughout the 0–250 Hz range.

Preliminary data analysis was performed as soon as the frequency response functions (FRFs) were available for processing. This allowed a quick study of the dynamic characteristics of the JWST OTE and also allowed the data quality to be verified through the use of coherence, complex mode-indicator functions (CMIFs), multivariate mode-indicator functions (MMIFs), power spectrum mode-indicator functions (PSMIFs), and FRF quality. Quick processing of the data into mode shapes permitted the MAC, orthogonality, and self-orthogonality to be computed between the test shapes, which helped to verify the independence of the extracted modes. Cross-orthogonality was also used to compare the test shapes to the analysis shapes.

An example drive point FRF and coherence plot for the stowed configuration is provided in Fig. 10.7. The drive point FRFs for all six shakers in the deployed configuration are provided in Fig. 10.8. As can be seen, the deployed configuration has a high modal density below 100 Hz. Linearity assessment was performed using the PSMIF. Because the PSMIF is the summation of all FRFs multiplied by each FRF conjugate, it is an ideal function to allow a global study of nonlinearity.

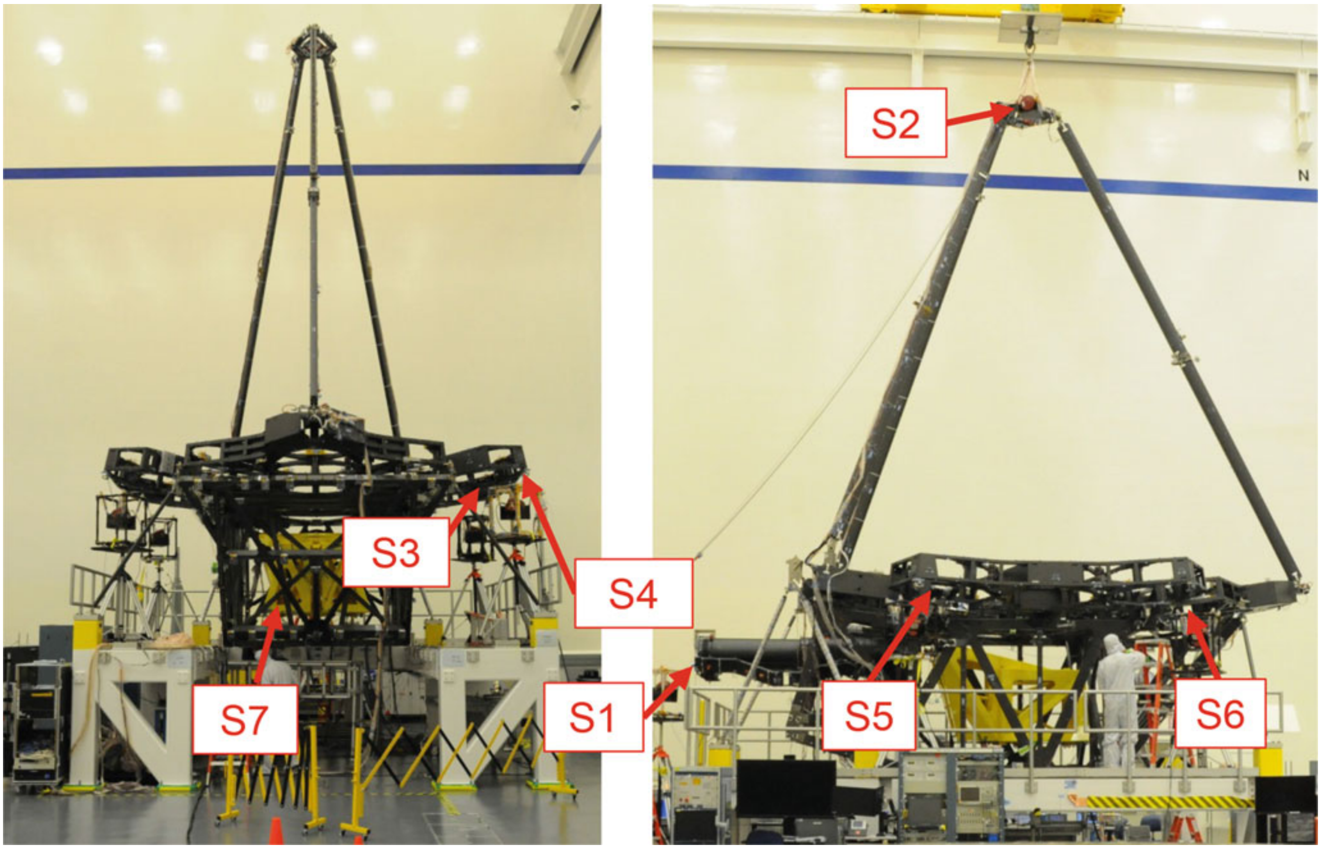

Fig. 10.6 Deployed configuration shaker locations

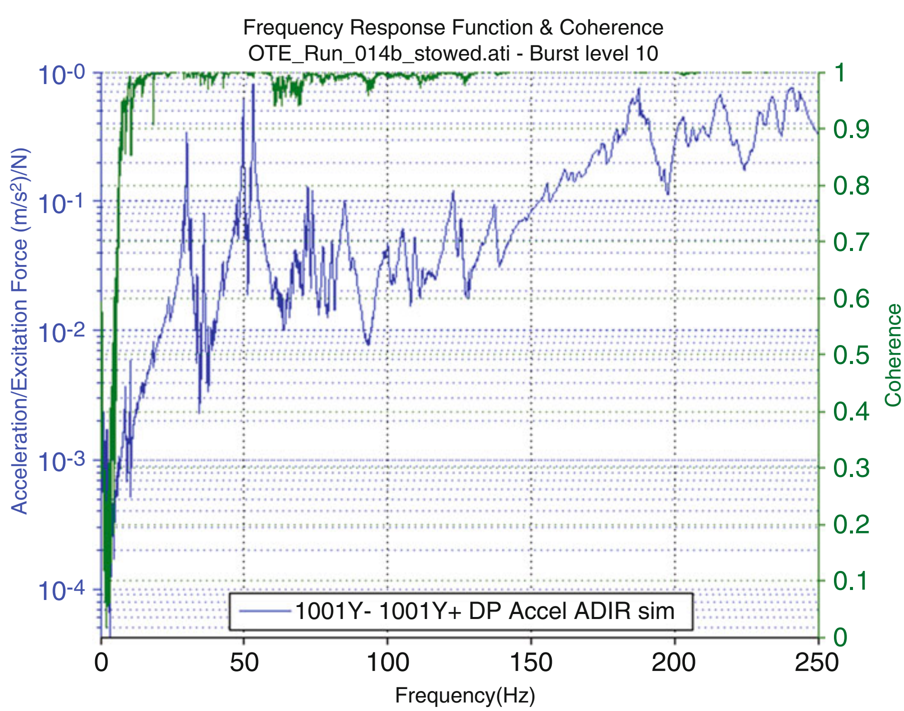

Fig. 10.7 Stowed configuration drive point FRF and coherence for one shaker, 0–250 Hz

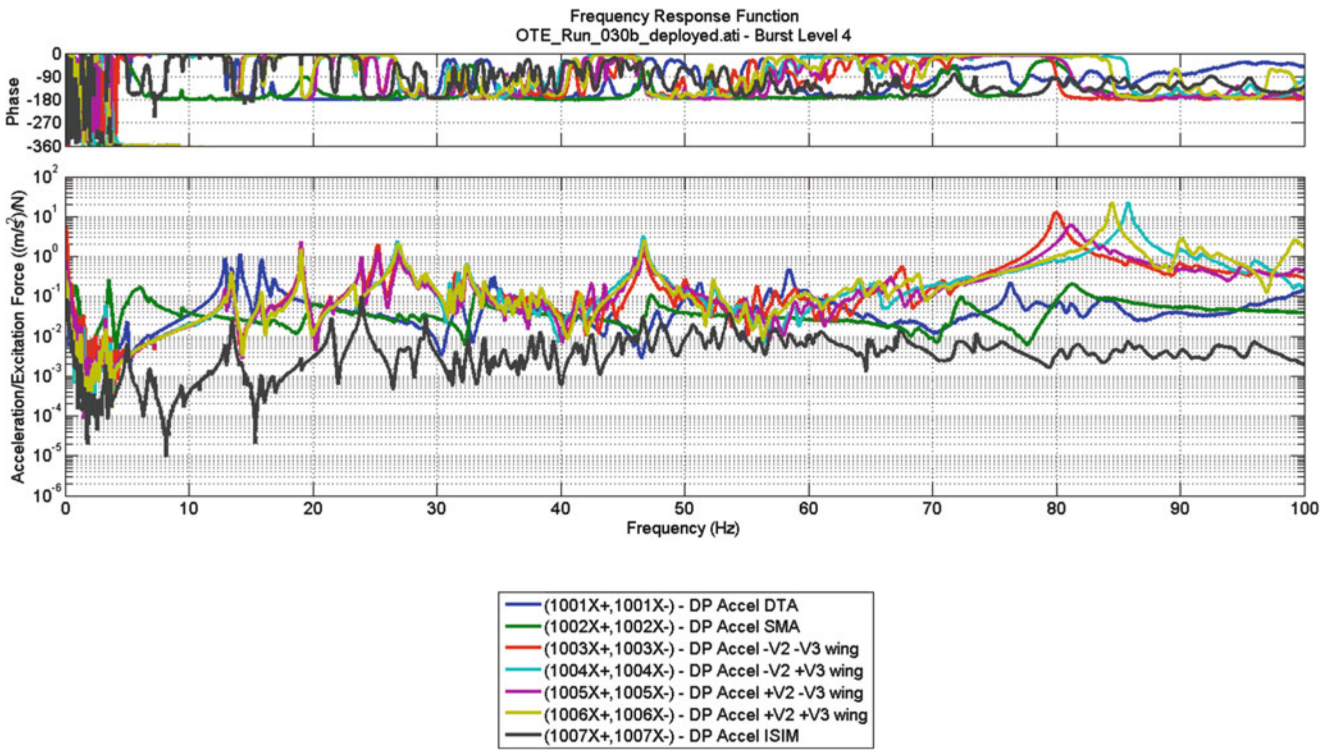

Fig. 10.8 Deployed configuration drive point FRFs, 0–100 Hz

10.4 Stowed Test Results

The stowed configuration test was performed first. During the test, it was noticed that the first bending mode in one direction was nonlinear and was 40 % below the analysis prediction. Fig. 10.9 shows the nonlinear response of the first mode. These PSMIF plots range from extremely low level (0.7 lbs RMS) to the highest level (7 lbs RMS). The nonlinear response and comparison to the analysis indicate that the support structure was not as stiff as preferred. A complete modal survey was completed, and while the test article was reconfigured for the deployed configuration, additional testing was performed on the stowed fixture to identify any differences in the stiffness from the prediction.

Initial modal impact testing of the fixture shows that there were differences in the stiffness of the four mounts. Figure 10.10 shows the three impact directions at each mount location to access and compare the stiffness. Figure 10.11 shows the drive point FRF in one direction at each of the 4 mounts. The acceleration/force (inertance) at low frequency is inversely proportional to stiffness. As can be seen in the overlay, one of the mounts is much stiffer than the other three. This quick modal test provided enough insight to show that the mounts were different. NGSC then performed additional static testing to experimentally measure the mount stiffness, which was then used to update the FEM used in the modal predictions. After this update, the analysis matched the test data within 20 % and the stowed configuration test was deemed complete. The static test was performed in parallel with the deployed configuration so that schedule was not affected.

A total of 76 modes were extracted up to 50 Hz for the stowed configuration. Using the static test data and updating the FEM predictions allowed the team to finalize the stowed configuration test without impacting schedule. The stowed configuration will be used to access launch loads. The higher-frequency content (above 40 Hz) is not critical for launch load assessment.

10.5 Deployed Test Results

The final mode set for the deployed configuration consisted of 188 modes up to 100 Hz. To get the best set of independent modes, several methods were implemented. First, five or six shakers were used simultaneously, providing burst-random input, and having multiple references allowed ATA to identify closely spaced modes using MMIF and CMIF plots. Second,

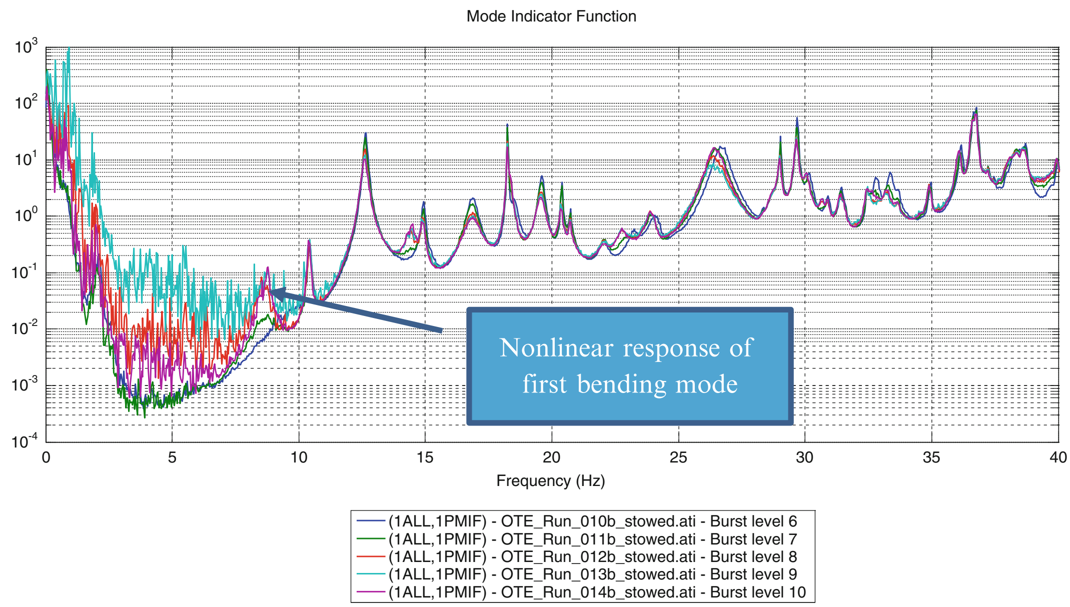

Fig. 10.9 Stowed PSMIF overlay to access linearity

Fig. 10.10 Fixture impact directions

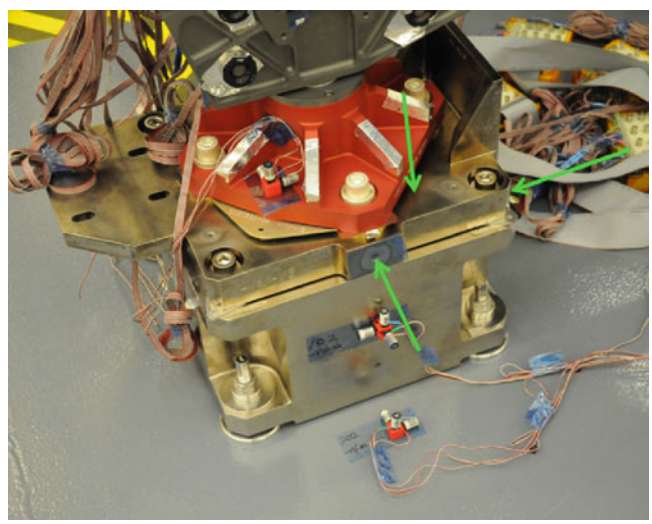

impact tests at each primary mirror simulator were combined into one data set. There were 18 locations in total, all very similar to each other, with closely spaced modes. By combining the FRFs from each location, a multi-reference impact data set was used to fit the frequency bands of the closely spaced modes. These modes were then combined with the burst-random modes and sorted for the best match to the analysis. Repeated modes were discarded. Photos of two locations are shown in Fig. 10.12. The transfer functions between the primary mirrors and the secondary mirror were also an important measurement. These transfer functions will be used to evaluate the mirror performance and line of sight.

The third method was using multiple types of curve-fitting algorithms to obtain low off-diagonal terms in the orthogonality matrix. ATA's IMAT software and alias-free polyreference (AFpoly^{TM}) [2] were used as the primary curve-fitting algorithm. The off-diagonal terms in the test self-orthogonality matrix from modes from AFpoly were then reviewed. There were a couple frequency bands that contained higher off-diagonal terms than desired—for example between 33 and 37 Hz—but a method called mode enhancement [3] was used to provide better mode extraction and therefore reduce the off-diagonal terms.

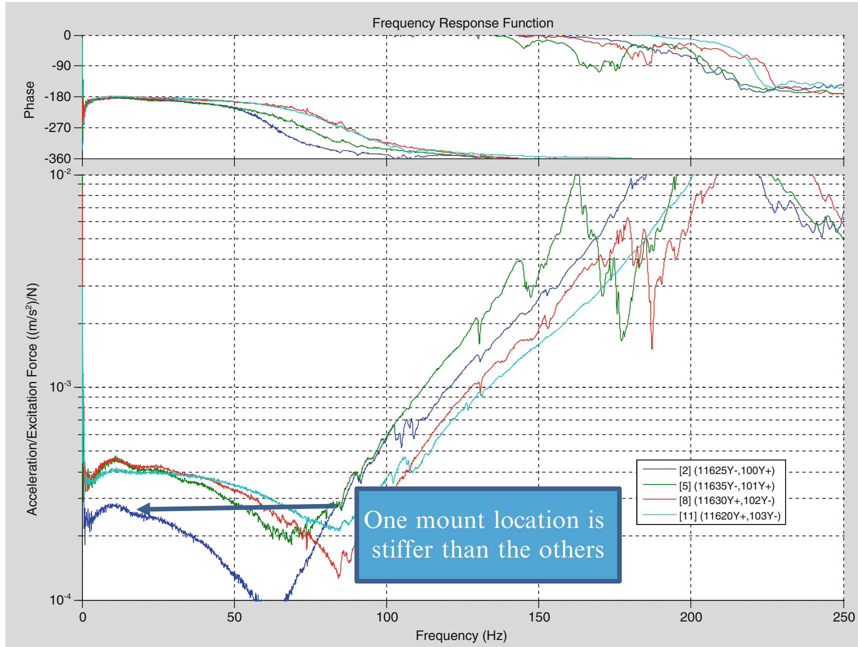

Fig. 10.11 Drive point inertance comparison

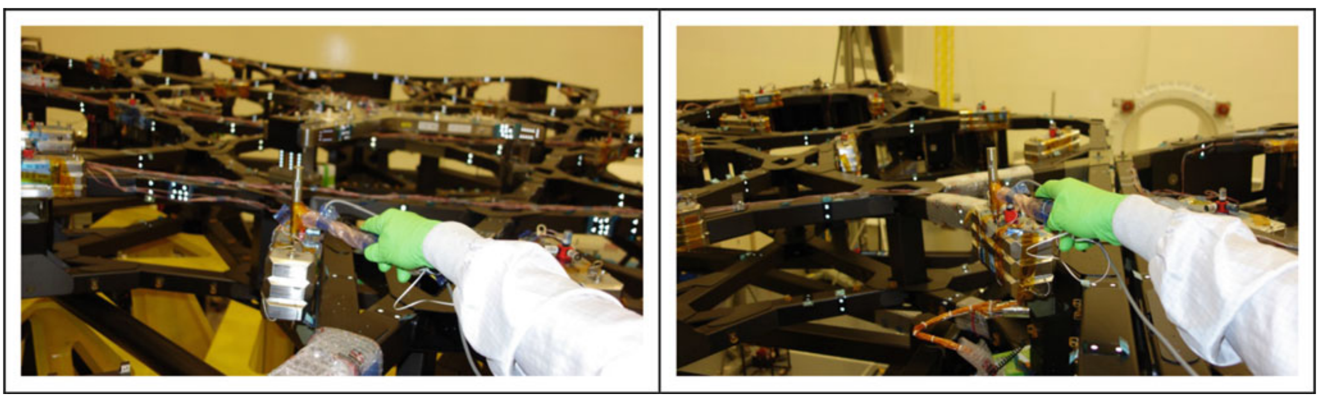

Fig. 10.12 Primary mirror mass simulator impacts—example photos of two locations

Mode enhancement techniques using the MMIF and/or CMIF were used to extract modes that were difficult to extract using AFPoly™ and other algorithms. These included bands of modes where there were high levels of modal coupling as defined by high off-diagonal terms in the test self-orthogonality matrix, and frequencies where the synthesized FRFs from modes extracted by AFPoly™ did not match the test data well. In the following example, the 36–38 Hz region contained a high modal density and required mode enhancement. Mode enhancement techniques often work better for sets of test data with a large number of modes over a very small frequency range, such as the modes associated with local deformations of the primary mirror mass simulators. The eigenvectors associated with the minimum value of the MMIF for each mode are defined as the force patterns necessary to drive the structure into a normal mode. Figure 10.13 shows the MMIFs from the random five-shaker run for the stowed configuration. The FRF matrix was post-multiplied by these force patterns to generate a set of mode-enhanced FRFs. The imaginary part of the resulting FRF matrix at resonance is assumed to be the mode shape as it would be for a mode extracted using a normal mode tuning technique. The FRF matrix is then pre-multiplied by this shape to create a single enhanced FRF. The measured drive point FRF and the enhanced FRF are compared in Figs. 10.14 and 10.15, showing that the modes in the 36–38 Hz range are much more prevalent after the enhancement. Damping and natural frequency values were extracted from the enhanced FRF. Figure 10.16 shows the enhanced FRF and the curve-fit data for the first two modes in this frequency range.

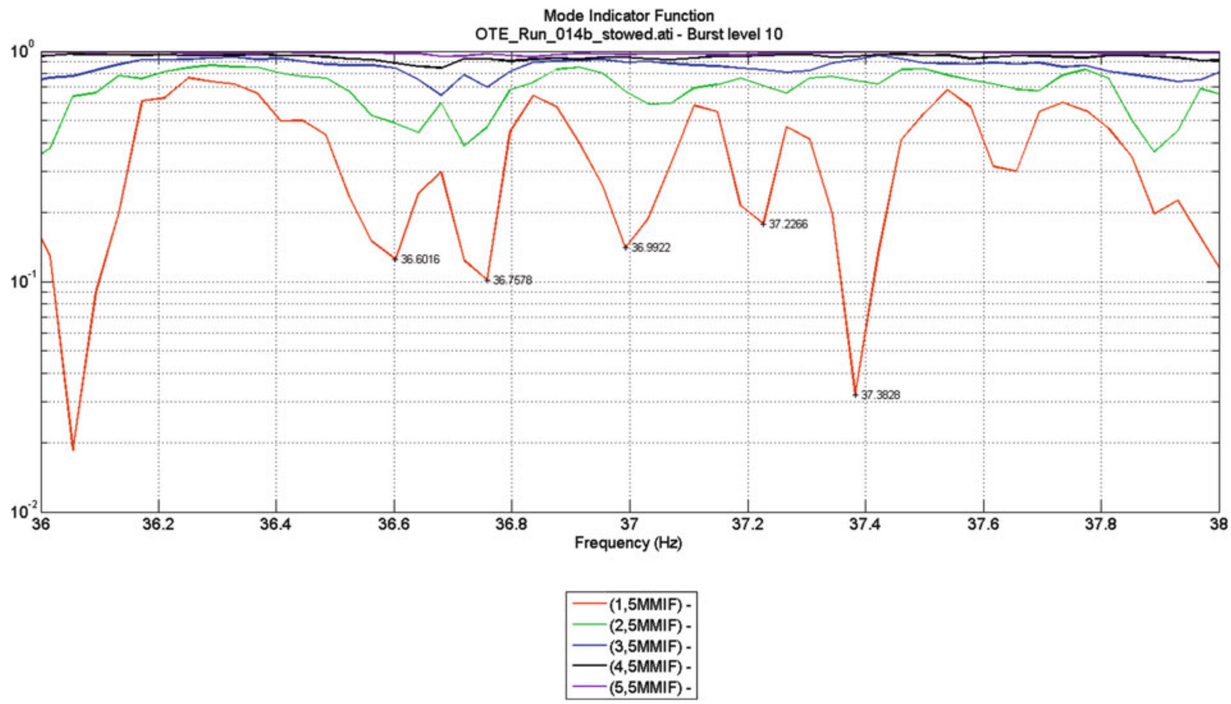

Fig. 10.13 MMIFs used to tag frequencies for mode enhancement

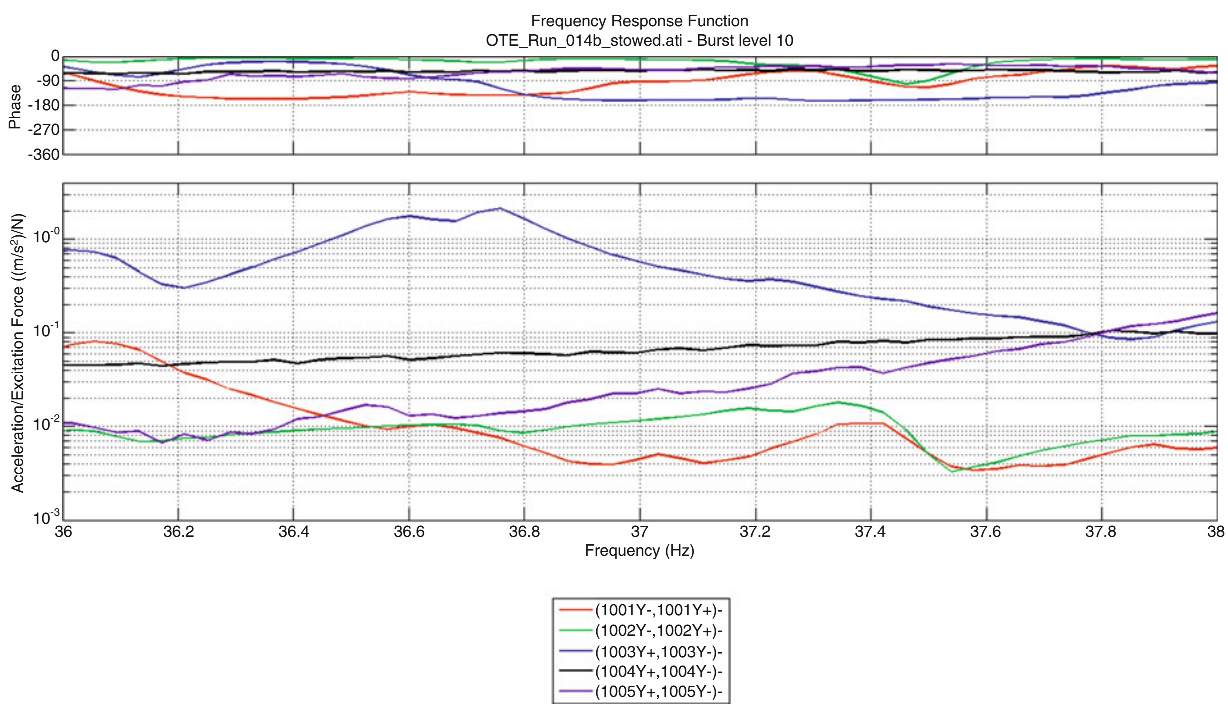

Fig. 10.14 Drive point FRF 36–38 Hz

The self-orthogonality tables are provided in Table 10.1 for the modes from 33 to 37 Hz. The table on the left was created using the measured FRF to perform the curve fits. The table on the right was created using the mode enhancement curve-fitting method. As can be seen in the table, just performing mode enhancement curve fitting reduced the off-diagonal terms by obtaining better mode shape fits from the data. This mode enhancement was repeated for other narrow frequency bands with a high number of modes.

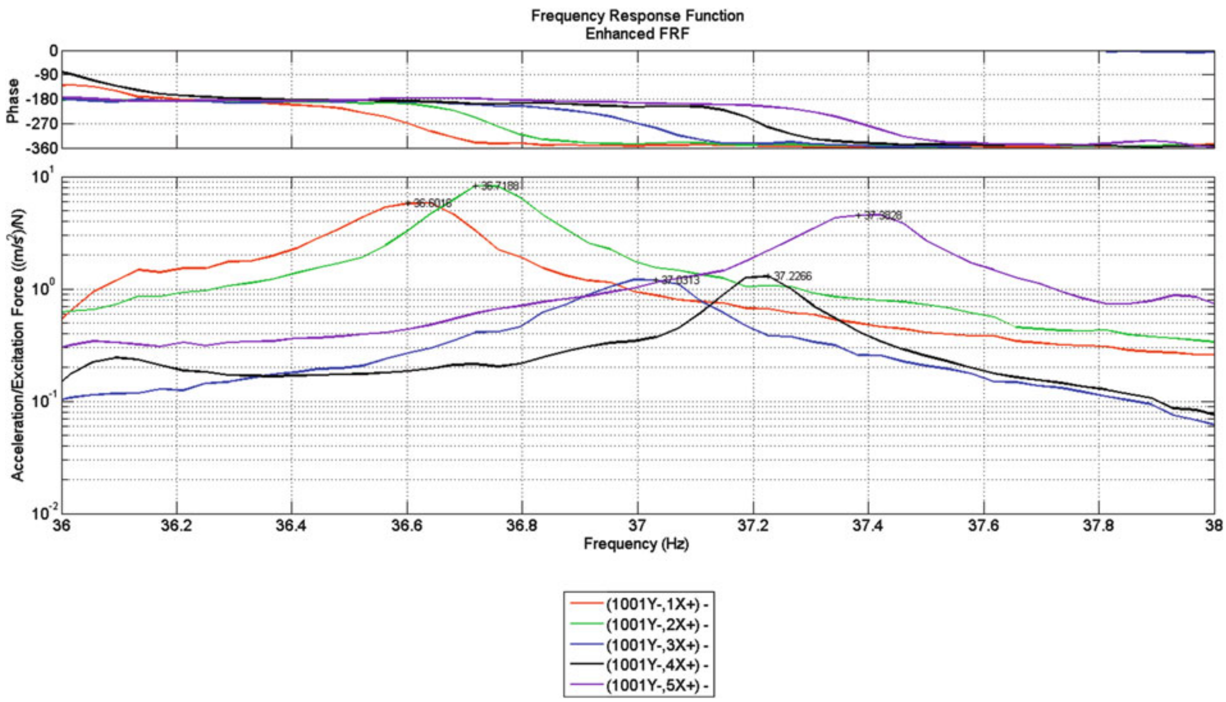

Fig. 10.15 Enhanced FRF 36–38 Hz

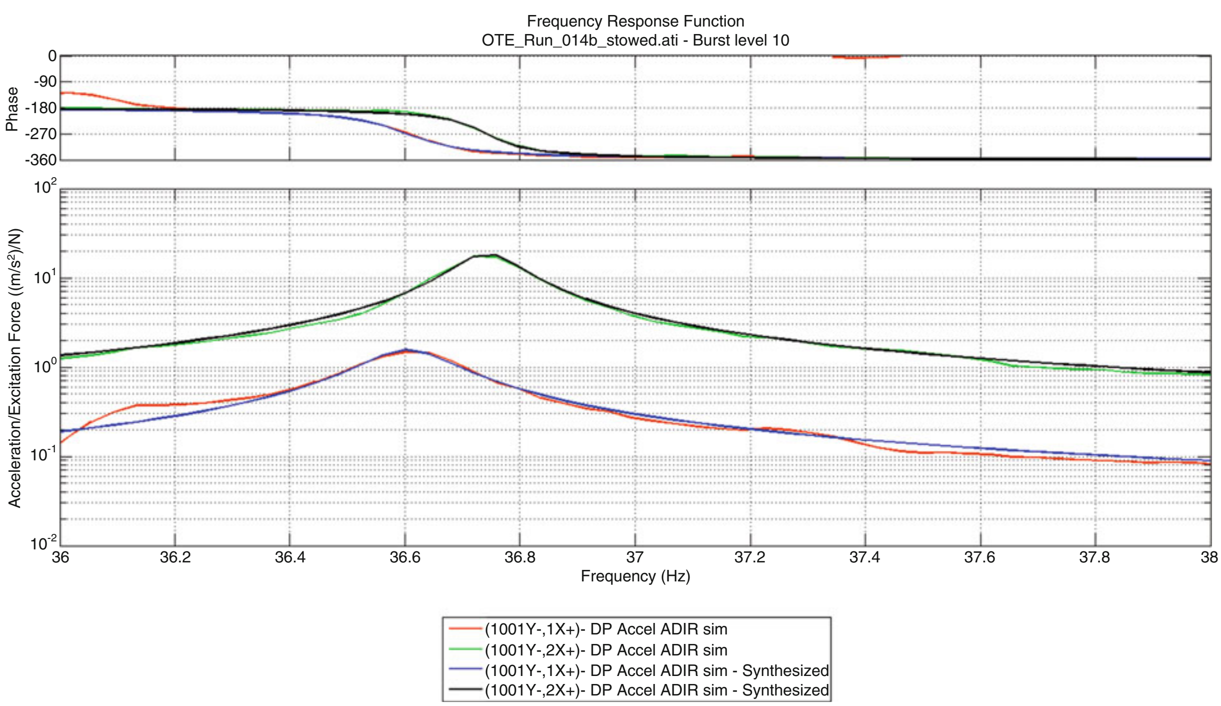

Fig. 10.16 FRF curve fit to enhanced FRF—first two modes shown

The typical fourth step in obtaining the best data for a spacecraft with high modal density is to use impact testing to excite modes that cannot be well excited from the shakers. These could be local component modes that are isolated from the main structure. In this case, the shakers were well placed, so impact testing to identify additional modes was not necessary.

The final self-orthogonality table up to 40 Hz is provided in Table 10.2. As can be seen, low off-diagonals were obtained using the methods and techniques described above. There were two areas where coupling of modes was observed. The first

Table 10.1 Self-orthogonality tables before (left) and after (right) mode enhancement curve fitting

Test Self Orthogonality Table

Test Shapes

		35	36	37	38	39	40	41	42	43	44	45
	Ott	33.8	34.6	35.0	35.5	35.6	35.7	35.8	36.1	36.3	36.7	36.8
35	33.8	1.00										0.06
36	34.6		1.00	0.13	0.07	0.09				0.09	0.08	0.06
37	35.0		0.13	1.00	0.06							
38	35.5		0.07	0.06	1.00	0.44	0.07	0.13				
39	35.6		0.09		0.44	1.00	0.08	0.06	0.07	0.06	0.11	
40	35.7				0.07	0.08	1.00					
41	35.8				0.13	0.06		1.00	0.19		0.10	
42	36.1					0.07		0.19	1.00	0.08	0.09	
43	36.3		0.09			0.06			0.08	1.00	0.16	0.05
44	36.7		0.08			0.11		0.10	0.09	0.16	1.00	0.14
45	36.8	0.06	0.06							0.05	0.14	1.00

Test Self Orthogonality Table

Test Shapes

		35	36	37	38	39	40	41	42	43	44	45
	Ott	33.8	34.6	35.0	35.4	35.6	35.7	35.9	36.1	36.3	36.6	36.8
35	33.8	1.00										0.08
36	34.6		1.00	0.09	0.05	0.08		0.06		0.07	0.08	0.07
37	35.0		0.09	1.00								
38	35.4		0.05		1.00	0.07	0.07	0.07				0.06
39	35.6		0.08		0.07	1.00	0.08	0.06				
40	35.7				0.07	0.08	1.00				0.05	
41	35.9		0.06		0.07	0.06		1.00	0.08	0.05	0.11	
42	36.1							0.08	1.00		0.09	
43	36.3		0.07					0.05		1.00	0.13	
44	36.6		0.08				0.05	0.11	0.09	0.13	1.00	0.08
45	36.8	0.08	0.07		0.06						0.08	1.00

Table 10.2 JWST OTE deployed final test modes: self-orthogonality (59 modes from 0 to 40 Hz)

Modes 1-59 from 0-40 Hz

Test Self Orthogonality Table

Test Shapes

TMD Mode

Modes 16, 17 coupled with SMSS torsion mode

Test Shapes		1	2	3	4	5	6	7	8	9	10	11	12	13	14	15	16	17	18	19	20	21	22	23	24	25	26	27	28	29	30
	Ott	3.3	3.6	4.8	5.0	5.4	6.1	6.8	9.4	11.7	12.9	13.4	13.5	14.0	15.8	16.6	16.8	17.4	19.0	21.5	23.3	23.9	25.2	26.8	27.0	27.7	28.8	29.1	31.0	31.5	31.7
1	3.3	1.00																													
2	3.6		1.00			0.07											0.08	0.14													
3	4.8			1.00	0.10	0.85	0.44																								
4	5.0			0.10	1.00	0.09											0.08	0.16													
5	5.4		0.07	0.85	0.09	1.00	0.08	0.05																							
6	6.1			0.44		0.08	1.00	0.08										0.06													
7	6.8					0.05	0.08	1.00									0.16	0.34													
8	9.4								1.00								0.21	0.42													
9	11.7									1.00																					
10	12.9										1.00				0.05																
11	13.4											1.00	0.06																		
12	13.5											0.06	1.00																		
13	14.0													1.00																	
14	15.8										0.05				1.00	0.05	0.05														
15	16.6														0.05	1.00		0.06													
16	16.8		0.08		0.08			0.16	0.21						0.05		1.00	0.08													
17	17.4		0.14		0.16		0.06	0.34	0.42							0.06	0.08	1.00													
18	19.0																		1.00												
19	21.5																			1.00											
20	23.3																				1.00	0.06									
21	23.9																				0.06	1.00									
22	25.2																						1.00								
23	26.8																							1.00		0.06					
24	27.0																								1.00	0.08					
25	27.7																							0.06	0.08	1.00					
26	28.8																										1.00				
27	29.1																											1.00			
28	31.0																												1.00		
29	31.5																													1.00	
30	31.7																														1.00
31	31.8																														
32	32.4																														
33	32.5																														
34	33.1																														
35	33.8																														
36	34.6																														
37	35.0																														
38	35.4																														
39	35.6																														
40	35.7																														
41	35.9																														
42	36.1																														
43	36.3																														
44	36.6																														
45	36.8																														
46	37.1																														
47	37.4																														
48	37.6																														
49	37.8																														
50	38.0																														
51	38.4																														
52	38.5																														
53	38.7																														
54	39.0																														
55	39.4																														
56	39.4																														
57	39.6																														
58	39.7																														
59	39.8																														

Test Shapes		31	32	33	34	35	36	37	38	39	40	41	42	43	44	45	46	47	48	49	50	51	52	53	54	55	56	57	58	59
	Ott	31.8	32.4	32.5	33.1	33.8	34.6	35.0	35.4	35.6	35.7	35.9	36.1	36.3	36.6	36.8	37.1	37.4	37.6	37.8	38.0	38.4	38.5	38.7	39.0	39.4	39.4	39.6	39.7	39.8
1	3.3																													
2	3.6																													
3	4.8																													
4	5.0																													
5	5.4																													
6	6.1																													
7	6.8																													
8	9.4																													
9	11.7																													
10	12.9																													
11	13.4																													
12	13.5																													
13	14.0																													
14	15.8																													
15	16.6																													
16	16.8																													
17	17.4																													
18	19.0																													
19	21.5																													
20	23.3																													
21	23.9																													
22	25.2																													
23	26.8																													
24	27.0																													
25	27.7																													
26	28.8																													
27	29.1																													
28	31.0																													
29	31.5																													
30	31.7																													
31	31.8	1.00																												
32	32.4		1.00	0.13																										
33	32.5		0.13	1.00																										
34	33.1				1.00																									
35	33.8					1.00										0.08														
36	34.6						1.00	0.09	0.05	0.08		0.06		0.07	0.08	0.07						0.08								
37	35.0						0.09	1.00										0.05												
38	35.4						0.05		1.00	0.07	0.07	0.07				0.06												0.05		
39	35.6						0.08		0.07	1.00	0.08	0.06																		
40	35.7								0.07	0.08	1.00				0.05									0.05			0.06			
41	35.9						0.06		0.07	0.06		1.00	0.08	0.05	0.11					0.06										
42	36.1											0.08	1.00		0.09															
43	36.3						0.07					0.05		1.00	0.13															
44	36.6						0.08				0.05	0.11	0.09	0.13	1.00	0.08														
45	36.8					0.08	0.07		0.06						0.08	1.00														
46	37.1																1.00										0.05			
47	37.4							0.05										1.00												
48	37.6																		1.00	0.08			0.05							
49	37.8											0.06							0.08	1.00	0.07									
50	38.0																			0.07	1.00									
51	38.4						0.08															1.00	0.28		0.07					
52	38.5																		0.05			0.28	1.00	0.28				0.09	0.06	0.06
53	38.7										0.05												0.28	1.00	0.27				0.05	
54	39.0																					0.07		0.27	1.00	0.08	0.05	0.13		0.08
55	39.4																								0.08	1.00		0.29		
56	39.4										0.06						0.05								0.05		1.00	0.44		0.20
57	39.6								0.05														0.09		0.13	0.29	0.44	1.00	0.08	0.73
58	39.7																						0.06	0.05				0.08	1.00	0.07
59	39.8																						0.06		0.08		0.20	0.73	0.07	1.00

was the TMDs near 5 Hz. The model did not include the TMD modes, so the mass matrix did not include the TMDs. The TMD mode couples with the main strut modes, per their design. The second set of modes that coupled was with a strut torsion mode: there was a single accelerometer mounted off the centerline of the single main strut, and this single DOF picked up the torsion mode of the strut. Since there was only one DOF, the mode shape was not completely defined and coupled with other strut modes.

An example mode shape, mode 11 at 13.39 Hz, is provided in Fig. 10.17 for the deployed configuration. Mode shapes were fairly well defined up to 40 Hz. Beyond this range, shapes were computed up to 100 Hz and will be used in performance calculations. As part of the final check of the mode fit quality, FRFs were synthesized using the final mode shapes. These computed FRFs were then compared to the measured FRFs. The first three orders of the CMIF overlay between the synthesized FRFs and the measured FRFs are provided in Fig. 10.18 up to 100 Hz. The closely matched CMIFs verify quality mode extractions.

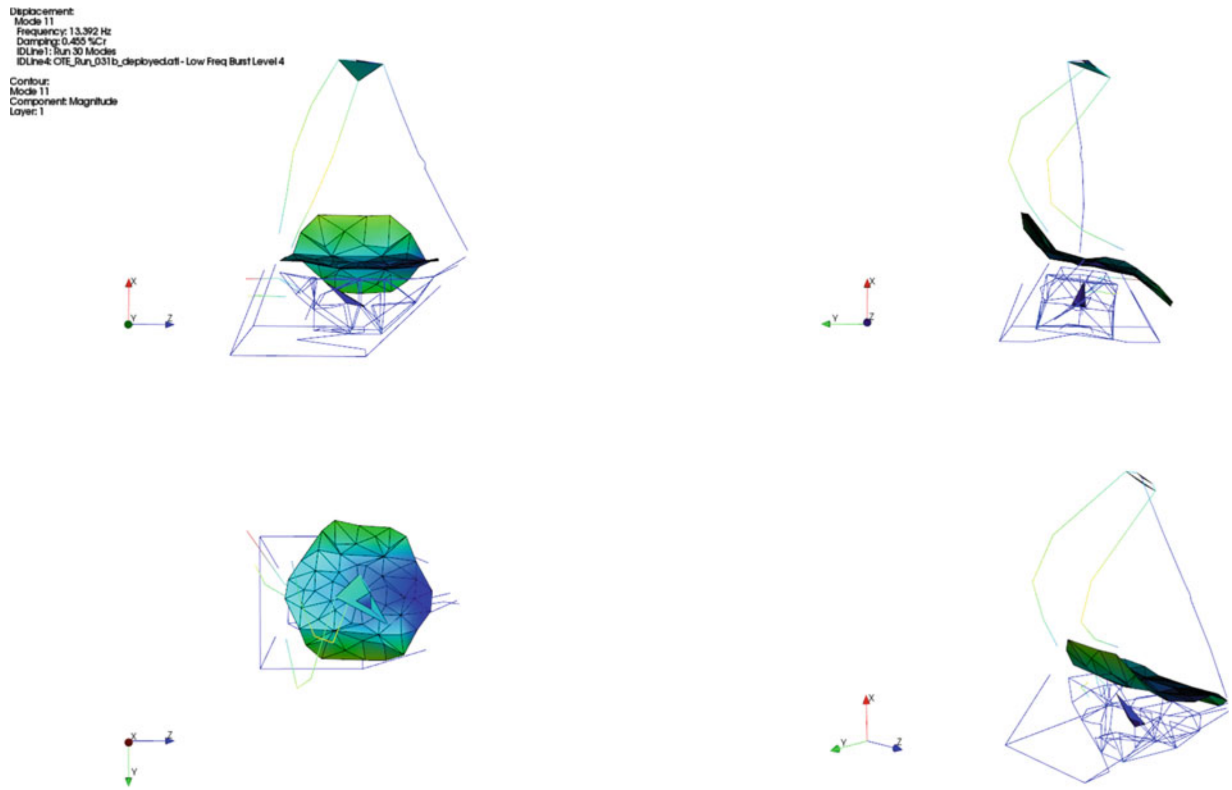

Fig. 10.17 Example mode shape of the deployed OTE

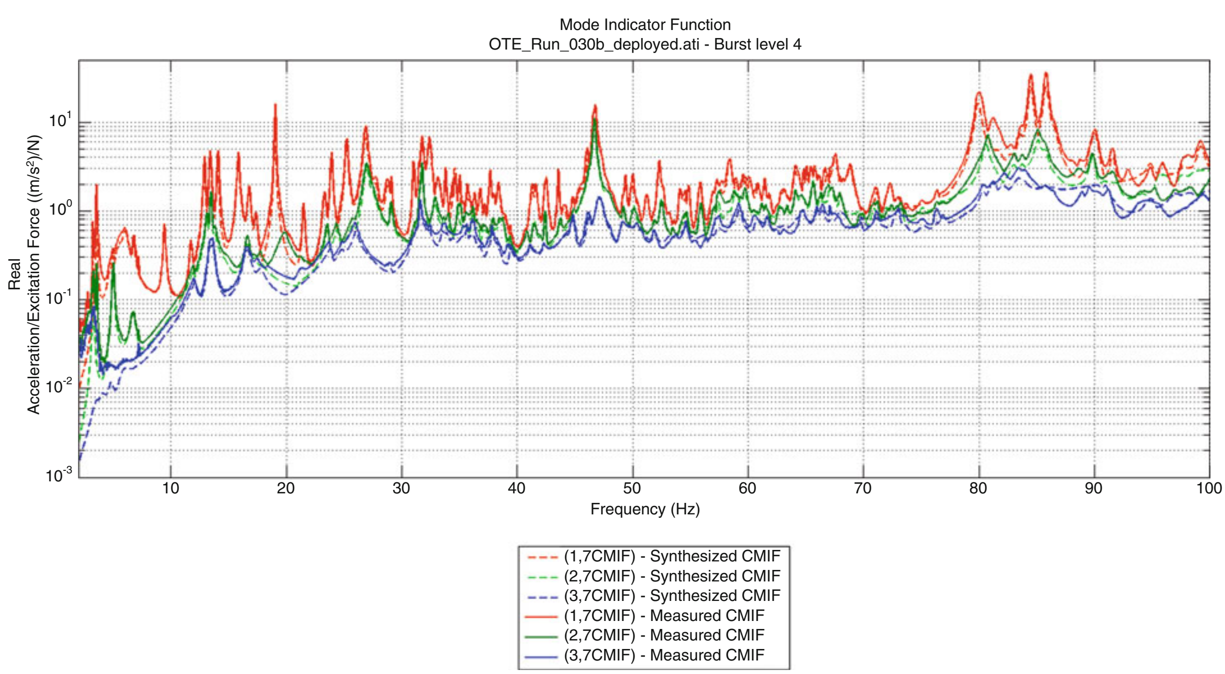

Fig. 10.18 Synthesized CMIF and measured CMIF used to verify mode shape extraction quality

10.6 Summary

The JWST OTE structure is a large and complex spacecraft. With proper test planning and execution and on-the-fly analysis, the modal test was successfully performed, obtaining critical transfer functions out to 250 Hz and modal parameters up to 100 Hz. This modally dense structure has several frequency bands with closely spaced modes, and several techniques were used to identify and verify unique modes. The fixture interface for the stowed configuration posed challenges; however, these were overcome by performing testing and analysis in parallel with those for the deployed configuration.

References

1. Brillhart, R., Dillion, M.: Automated test setup in modal testing. In: 10th International Modal Analysis Conference, Los Angeles, CA, February 2002
2. Brillhart, R., Napolitano, K., Osterholt, D.: Utilization of alias free polyreference for mixed mode structures. In: 26th International Modal Analysis Conference, Orlando, FL, February 2008
3. Napolitano, K.: Using FRF interpolation to help separate closely spaced modes. In: 24th International Modal Analysis Conference, St. Louis, MO, 2006